

Coherent seasonal acceleration of the Weddell Sea boundary current system driven by upstream winds

Nicolas Le Paih¹, Tore Hattermann^{2,1}, Olaf Boebel¹, Torsten Kanzow^{1,3}, Christof Lüpkes¹, Gerd Rohardt¹, Volker Strass¹, Steven Herbette⁴

¹Alfred Wegner Institute, Germany

²Norwegian Polar Institute, Norway

³Bremen University, Germany

⁴Laboratoire d'Océanographie Physique et Spatiale (LOPS), IUEM, Univ. Brest, CNRS, IRD, Ifremer, France

Contents

1. Text S1 to S2
2. Figure S1 to S4

Text S1 : Details on the optimal interpolation (OI)

To perform the OI, the dataset is split into sub-datasets corresponding to vertical subdomains. Although this choice is somehow arbitrary, choosing subdomains of 10 m (10-80 m) layer thickness for the constant vertical (terrain-following) coordinates ensures to have a well-resolved interpolation grid and, include enough data to limit the error of the estimated field. The optimal interpolation is iteratively performed by depth-layers to produce map of temperature and salinity in the PPV-Z space. Points with an error larger than 0.1°C and 0.02 absolute salinity are discarded. Temperature (T) and salinity (S) are determined at each interpolation grid point (g) from a linear weighted combination of valid observations selected around the interpolation depth,

$$T_g, S_g(PPV, Z_i) = \overline{T, S} + w \cdot [T, S - \overline{T, S}]. \quad (1)$$

i is the depth index. $\overline{T, S}$ is the averaged value of the sub-dataset, corresponding to the first guess. The interpolation is weighted such that, the larger the difference on PPV and/or the larger the uncertainty on the data points, the smaller the weights (w).

Corresponding author: Nicolas Le Paih, nicolas.le.paih@awi.de

w are then defined as a function of, the PPV distance, the uncertainty associated to the instrument accuracy (ϵ) and, the uncertainty associated to the temporal variability of the measured field (η),

$$w = C_{dg} \cdot [C_{dd} + I \cdot (\epsilon^2 + \eta^2)]^{-1}. \quad (2)$$

I is the identity matrix. The PPV distances are enclosed in the data-grid (C_{dg}) and data-data (C_{dd}) covariance matrices. These matrices are filled with values of covariance between two points (a,b) based on a Gaussian decay law which depends on the point to point PPV distance [Böhme *et al.*, 2005],

$$C_{ab}^2 = \langle s^2 \rangle \exp\left(-\frac{|PPV_a - PPV_b|^2}{PPV_a^2 + PPV_b^2}\right). \quad (3)$$

with $\langle s^2 \rangle$ being the variance of the sub-dataset. It represents the variability to the mean state used to scale the covariance functions. ϵ corresponds to 1.10^{-3} °C and 2.10^{-3} PSU for the CTD profiles, to 2.10^{-3} °C and 1.10^{-2} PSU for the float profiles and to 2.10^{-2} °C and 3.10^{-2} PSU for the seal profiles. η^2 describes the variations between nearby data located within the same depth layer [Reeve *et al.*, 2016],

$$\eta^2 = \frac{1}{2N} \sum_{d=1}^N (x_d - x_n)^2 \quad (4)$$

x_d are the data points, x_n are their closest neighbour and N is total the number of points in the sub-dataset. The algorithm used for the OI is summarised in Figure step OI.

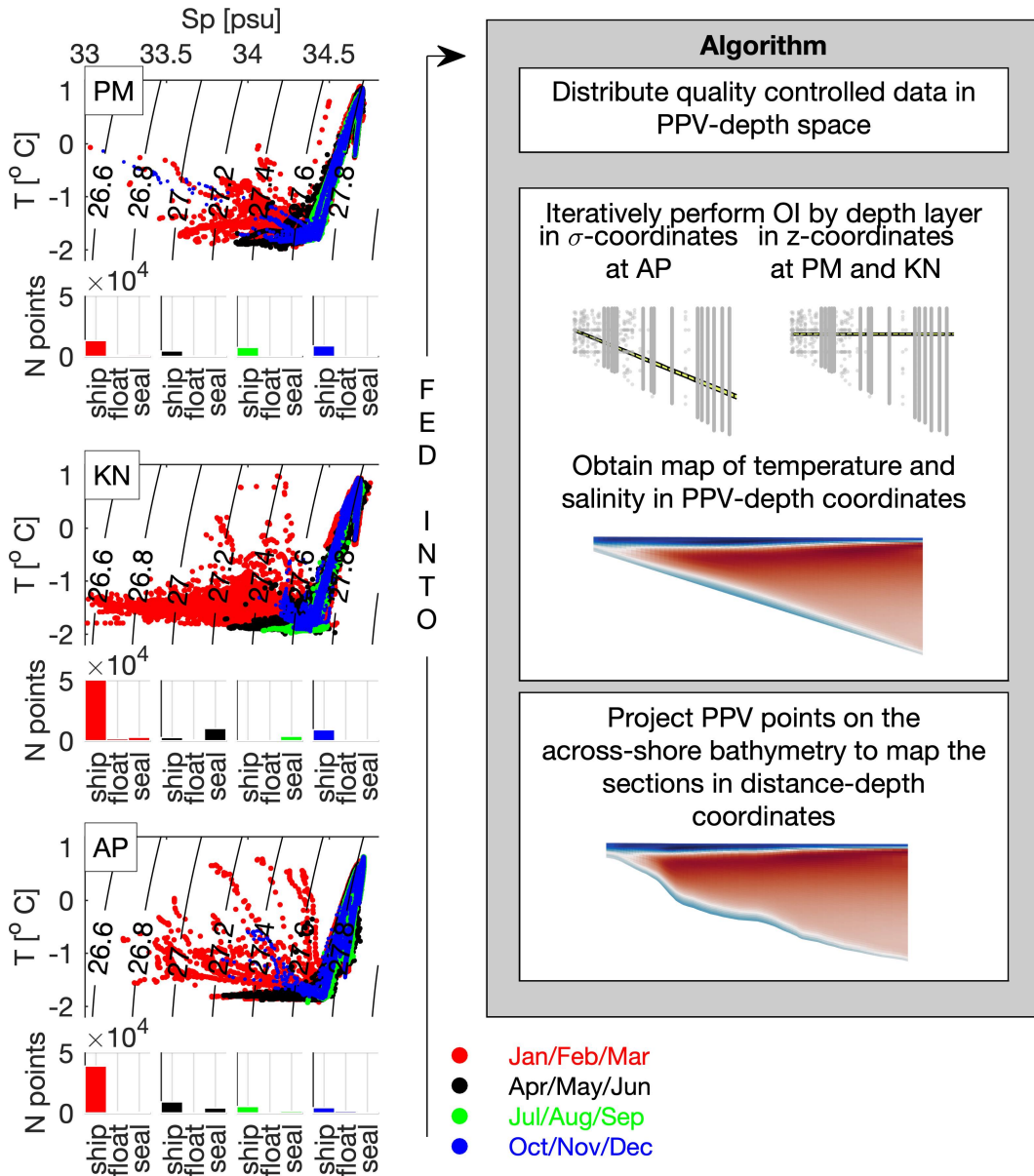


Figure step OI. T-S diagram of the data fed into the optimal interpolation (OI) at PM, KN and AP. The seasonal distribution of the data observed above 800 m depth and used for the OI is indicated below the T-S diagrams. Right panel) Algorithm used to construct the local sections.

Text S2 : Error associated to the vertical interpolation

The uncertainty associated to the seasonal variations of the barotropic velocity (u_{bt}) includes the error related to the calculation of the multi-year average of monthly means (σ_{err}) and, the error related to the vertical interpolation (σ_{pchip}),

$$\sigma_{bt} = \sqrt{\frac{1}{I} \sum_{i=1}^I \sigma_{err}^2(i) + \sigma_{pchip}^2}, \quad (5)$$

I being the number of multi year time series used to perform the depth-average. At each study location, σ_{pchip} is estimated from a set of realistic velocity profiles. This set includes all thermal-wind derived profiles estimated via objective mapping to represent a large range of realistic profiles. Each of them is normalized and velocities are interpolated between the current meter depths assuming a linear, spline or pchip interpolation method to model mooring profiles (Figure vertical interpolation). The difference between the depth-averaged velocity calculated from realistic and mooring profiles represents the uncertainty on u_{bt} associated to the vertical interpolation. This error was quadratically averaged within the set of profiles to estimate a typical error of interpolation at the three study sites. The pchip proved to perform the best, giving an error of 2%, 1.4% and 8.7% of the shear at PM_1 , KN_2 and AP_2 , respectively. Then, this error was scaled depending both on the seasonal shear and the study location and, included in σ_{bt} . Note that the error associated to the baroclinic velocities ($u_{bc} = u_i - u_{bt}$) corresponds to,

$$\sigma_{bc}(i) = \sqrt{\sigma_{err}^2(i) + \sigma_{bt}^2}. \quad (6)$$

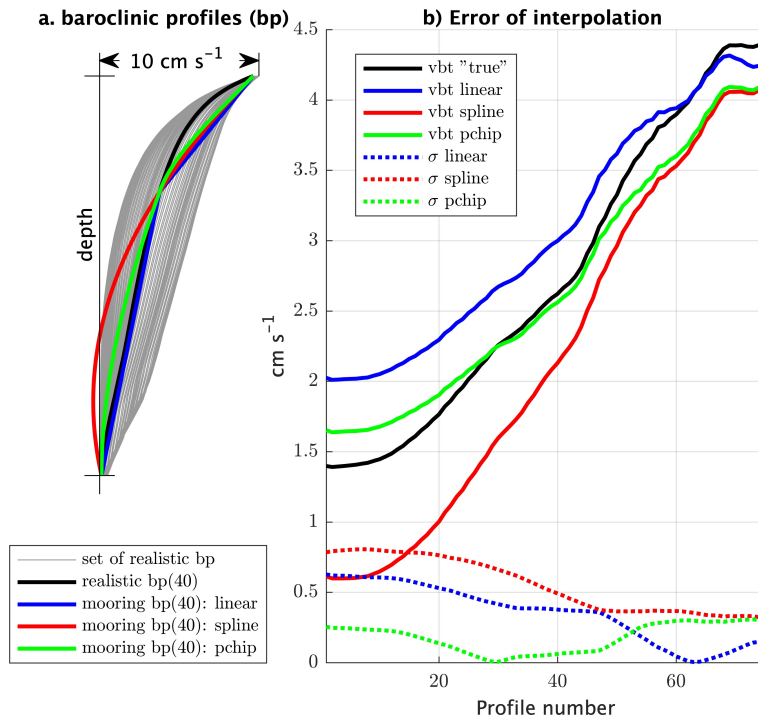


Figure vertical interpolation. a) Set of baroclinic profiles (bp) estimated at PM. Gray lines: realistic profiles. Black line: realistic profile number 40. Colored lines: mooring profiles estimated from the realistic profile number 40. b) Error of interpolation associated to each profile. Solid lines: baroclinic velocity depth-averaged (v_{bt}). Dotted lines: difference between realistic bp and mooring bp.

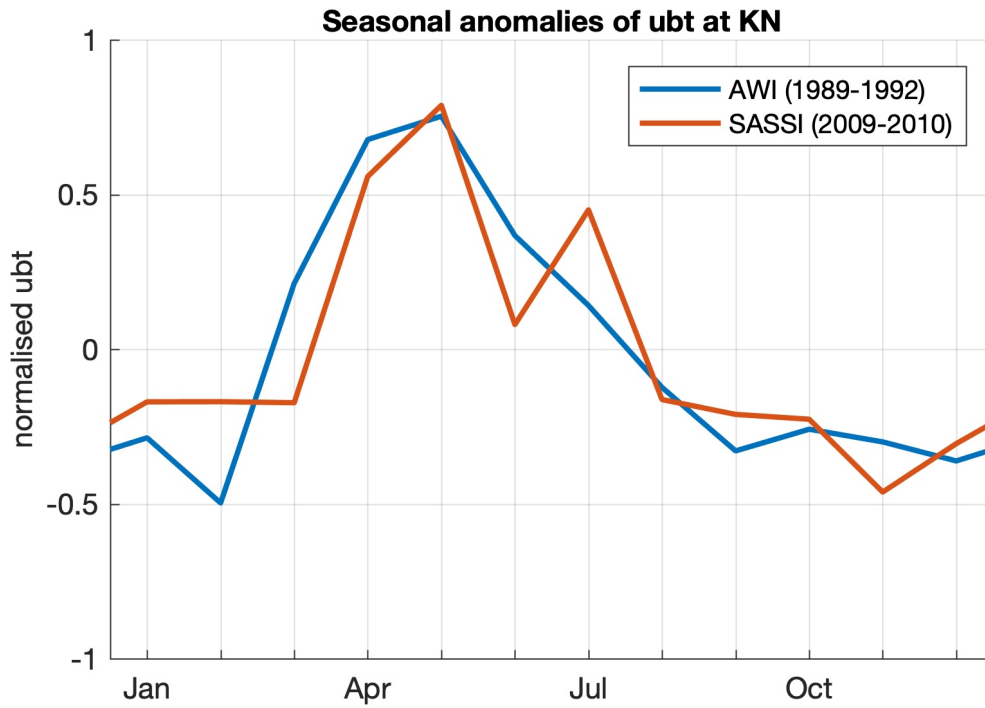


Figure S1. Phase of the barotropic flow (ubt) estimated over the 2500 isobath at Kapp Norvegia for different years from different mooring arrays. The AWI array has been deployed between 1989 and 1992 at 13°W (Fig. 1 and 2, main manuscript). The SASSI array has been deployed between 2009 and 2010, 350 km downstream of the former array (Graham et al., 2013).

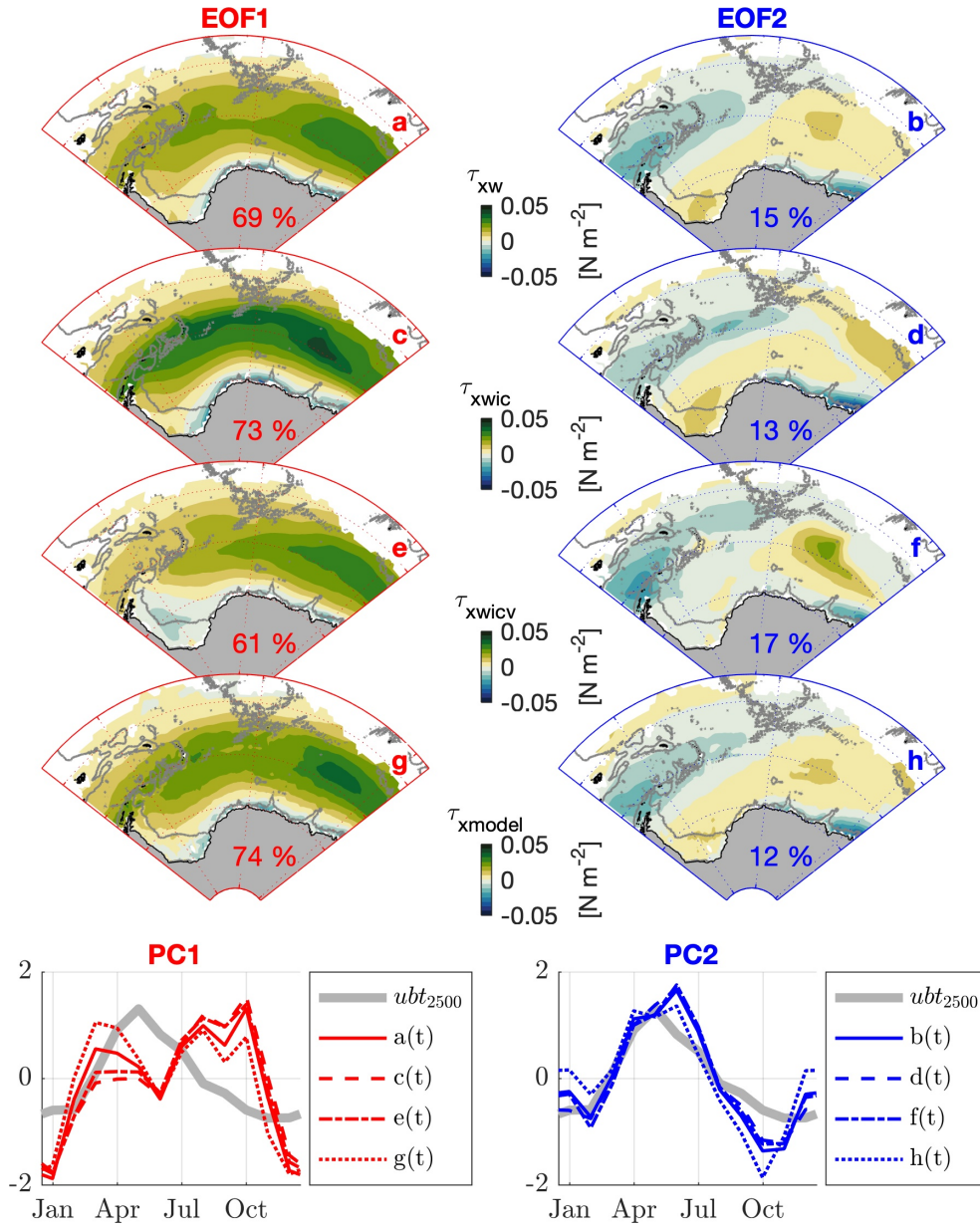


Figure S2. Comparison between the phase of the barotropic flow (ubt) estimated along the 2000-2500 m isobath and the two first modes of zonal stress. (a,b) Zonal stress estimated from τ_w . (c,d) Zonal stress estimated from τ_{wic} . (e,f) Zonal stress from τ_{wicv} . (g,h) Zonal stress estimated from τ_{model} . The percentage of variability explained by each mode is indicated. The bottom panels show the principal components of mode 1 and 2, from left to right. The definitions of τ are given in the main manuscript in Section 2.3.

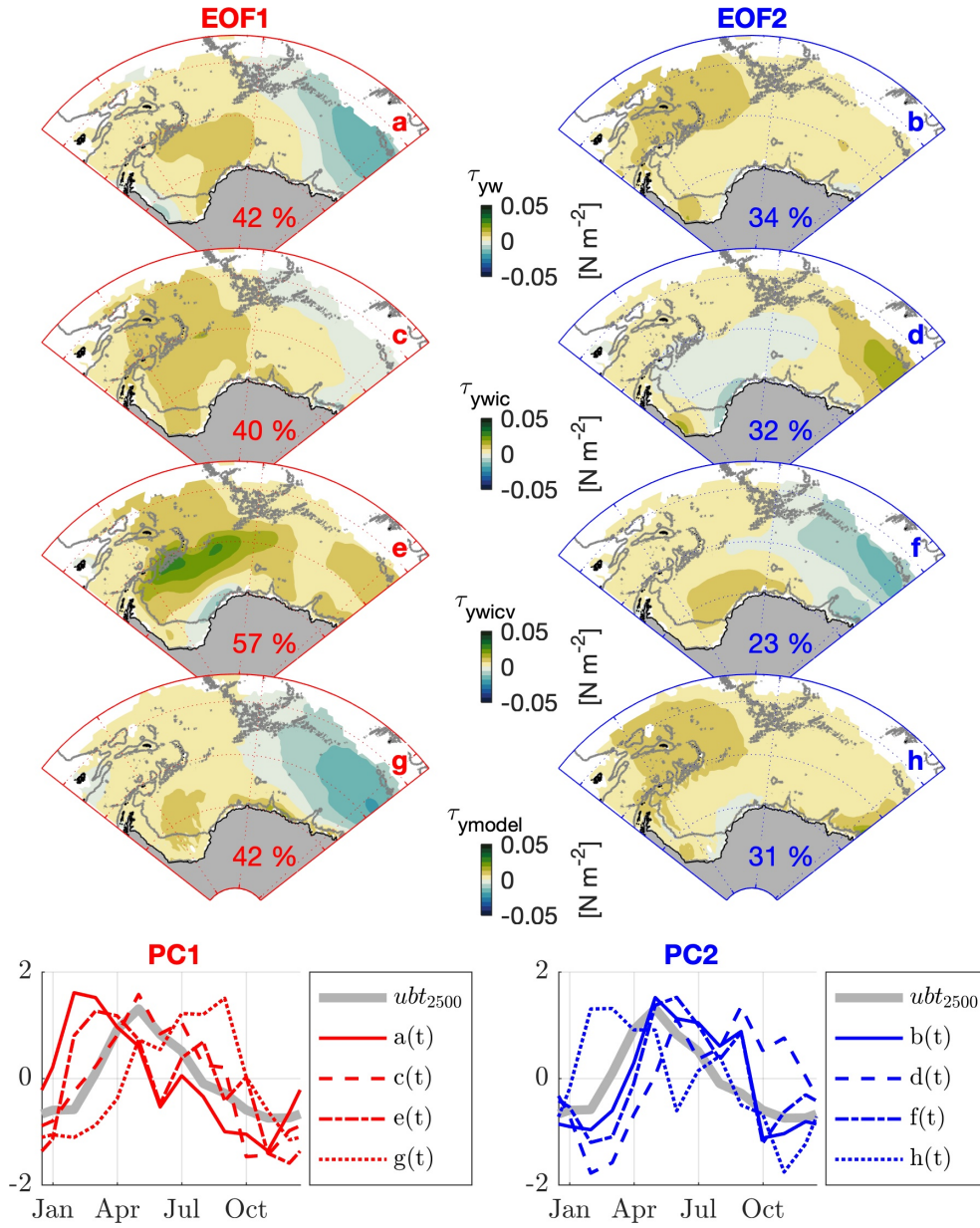


Figure S3. Comparison between the phase of the barotropic flow (ubt) estimated along the 2000-2500 m isobath and the two first modes of meridional stress. (a,b) Meridional stress estimated from τ_w . (c,d) Meridional stress estimated from τ_{wic} . (e,f) Meridional stress from τ_{wicv} . (g,h) Meridional stress estimated from τ_{model} . The percentage of variability explained by each mode is indicated. The bottom panels show the principal components of mode 1 and 2, from left to right. The definitions of τ are given in the main manuscript in Section 2.3.

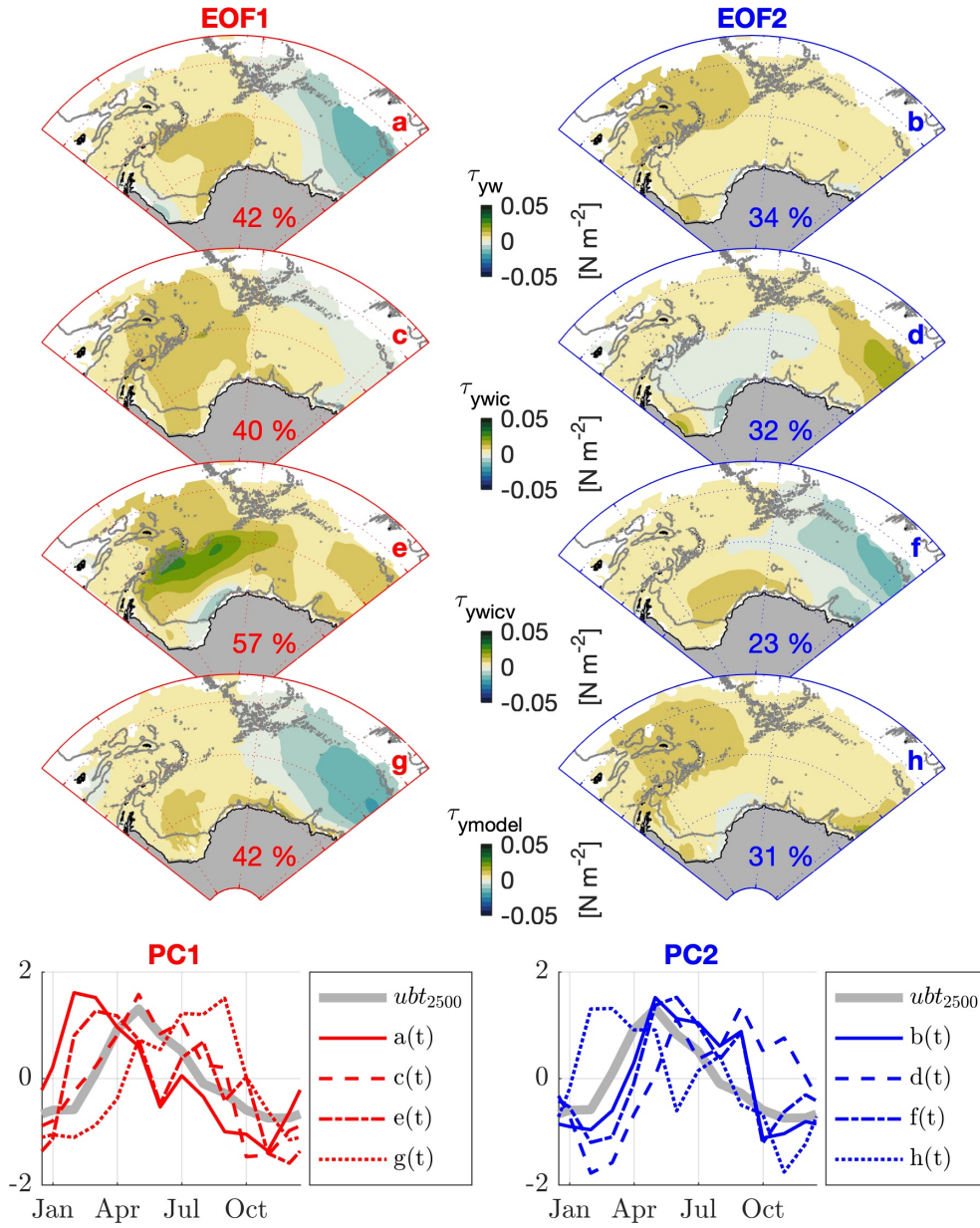


Figure S4. Comparison between the phase of the barotropic flow (ubt) estimated along the 2000-2500 m isobath and the two first modes of Ekman pumping. (a,b) Ekman pumping estimated from τ_w . (c,d) Ekman pumping estimated from τ_{wic} . (e,f) Ekman pumping from τ_{wicv} . (g,h) Ekman pumping estimated from τ_{model} . The percentage of variability explained by each mode is indicated. The bottom panels show the principal components of mode 1 and 2, from left to right. The definitions of τ are given in the main manuscript in Section 2.3.

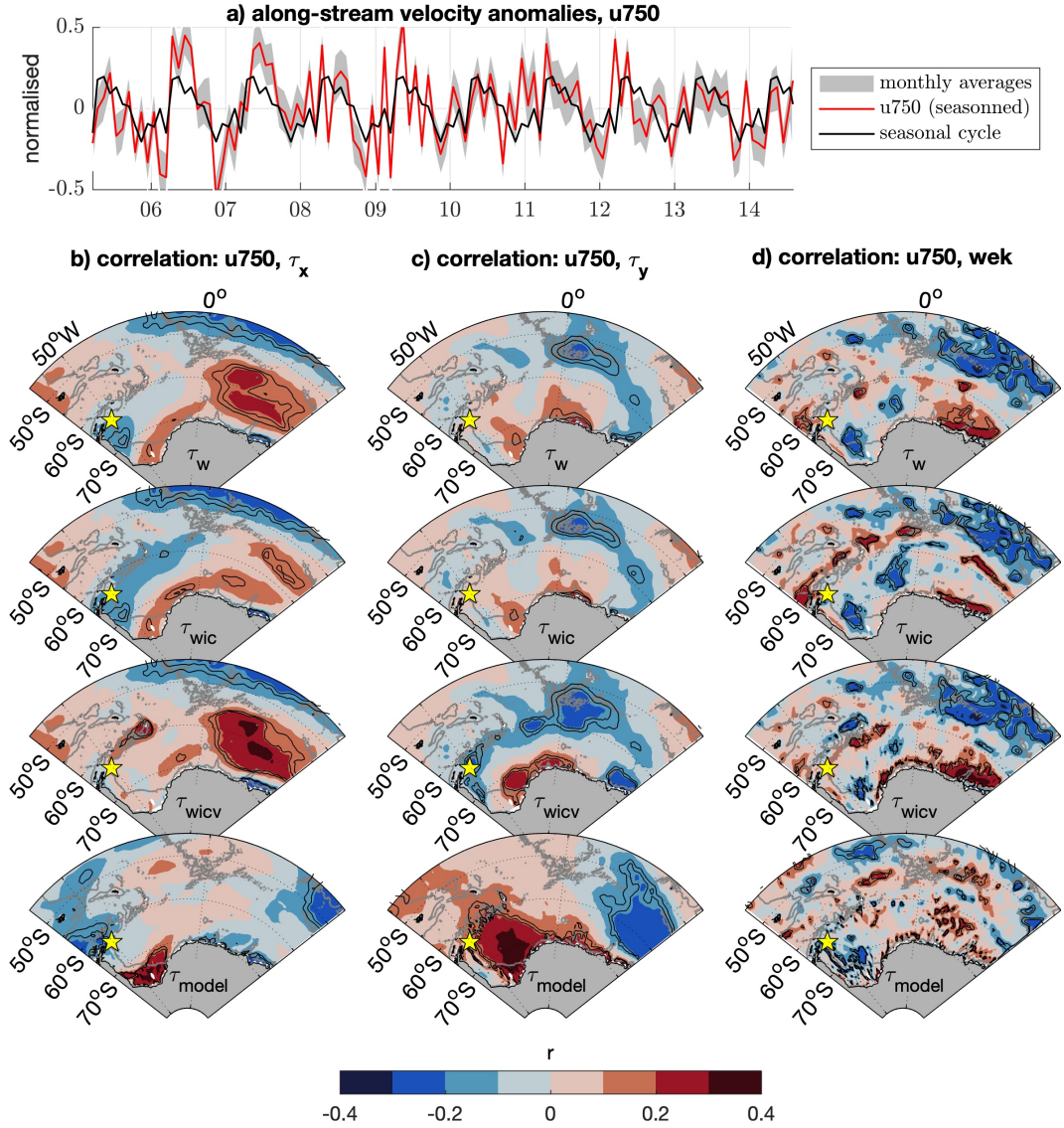


Figure S5. Two-months lag correlation between the monthly velocity observed between 2005 and 2015 at AP₂₅₀₀ and the different components of surface stress. The velocity at 750 m is used as a proxy for the barotropic variations. The correlations maps are computed for four different estimates of surface stress, τ_w , τ_{wic} , τ_{wicv} and τ_{model} , which are defined in the main manuscript in Section 2.3. a) monthly velocity at 750 m depth. b,c and d) Correlation between u750 and the zonal stress, meridional stress and Ekman pumping, respectively. The star shows the position of AP₂₅₀₀. The black contours represent 90 and 95 % confidence interval.